

Alkali-responsive membrane prepared by grafting dimethylaminoethyl methacrylate onto ethylene vinyl alcohol copolymer membrane

Hui Ye,^{1,2} Long Chen,^{1,2} Anni Li,^{1,2} Lilan Huang,^{1,2} YuZhong Zhang,^{1,2} Yingna Li,^{1,2,3} Hong Li^{1,2}

¹State Key Laboratory of Hollow Fiber Membrane Materials and Processes, Tianjin Polytechnic University, Tianjin 300387, China

²School of Materials Science and Engineering, Tianjin Polytechnic University, Tianjin 300387, China

³Department of Environmental and Chemical Engineering, Tangshan College, Tangshan 063000, People's Republic of China

Correspondence to: Y. Z. Zhang (E-mail: zhangyz2004cn@vip.163.com)

ABSTRACT: An alkali-responsive membrane was prepared by grafting dimethylaminoethyl methacrylate (DMAEMA) onto ethylene vinyl alcohol copolymer (EVAL) membrane using ultraviolet (UV) irradiation graft polymerization. A subtranslucent state of EVAL membrane swelling in the DMAEMA solution was observed, and such a state enabled the passage of UV light through all the pores, inducing graft polymerization inside the pores and on the back. Attenuated total reflectance Fourier-transform infrared spectrometer (ATR-FTIR), X-ray photoelectron spectroscopy (XPS), field-emission scanning electron microscopy (FESEM), and energy-dispersive X-ray spectroscopy (EDX) confirmed that the poly(DMAEMA)-grafted chains existed not only on the top surface, but also inside the pores and on the back. Atomic force microscopy (AFM) and nitrogen adsorption analysis confirmed that the grafted chains collapsed in air, and decreased the surface roughness, surface area, and pore size of the grafted membranes. Alkali-responsive properties of the poly(DMAEMA)-grafted EVAL membrane (i.e., contact angle, permeability, and selectivity) were observed in the pH range of 9–10. © 2014 Wiley Periodicals, Inc. *J. Appl. Polym. Sci.* **2015**, *132*, 41775.

KEYWORDS: grafting; membranes; stimuli-sensitive polymers

Received 14 June 2014; accepted 16 November 2014

DOI: 10.1002/app.41775

INTRODUCTION

The pH-responsive membranes can change in terms of physicochemical properties, mass transfer, and interfacial properties in response to changes in environmental pH.^{1,2} Such membranes are popular because of their useful applications in various fields, including sensors,³ separation processes,⁴ and drug and gene delivery devices.^{5,6} Surface-initiated graft polymerization is among the most widely used methods to create pH-responsive membranes with controlled permeability and selectivity, which involves grafting pH-responsive polymers onto porous membranes.

The most commonly used pH-responsive polymers comprise carboxyl and pyridine groups,^{7–10} which can change their chain configuration under acidic environmental conditions. Permeability and selectivity of these acid-responsive membranes can be regulated at pH values ranging from acidic to neutral. Regulation of these membranes is necessary to control chemical and drug release. However, few articles have reported on alkali-responsive membranes, which could potentially separate alkaline multicomponent mixtures. For example, soy protein concentrates are produced using a dilute alkali (pH 8–9) and contain various bioactive fractions, including soy protein, oligosaccha-

rides, flavonoids, and minerals.¹¹ In addition, traditional Chinese medicine (TCM) extracts are also alkaline multicomponent mixtures with high functional value.¹²

Poly(dimethylaminoethyl methacrylate) (PDMAEMA), a typical cationic polyelectrolyte, can ionize at high pH. Several researchers have grafted PDMAEMA onto membrane surfaces to prepare ion-exchange and antimicrobial membranes.^{13–15} Ethylene vinyl alcohol copolymer (EVAL), a semicrystalline random copolymer, comprises hydrophobic ethylene and hydrophilic vinyl alcohol segments; EVAL has become a promising biomedical material because of its excellent hydrophilicity and satisfactory biocompatibility.¹⁶ EVAL membranes have been widely used in blood purification devices, plasma protein separation,^{17,18} cell culture,^{19,20} drug delivery,^{21,22} and packaging applications. To our knowledge, EVAL membranes have not yet been functionalized with grafted stimuli-responsive polymers.

In this study, alkali-responsive EVAL membranes were initially prepared by grafting dimethylaminoethyl methacrylate (DMAEMA) using ultraviolet (UV) irradiation graft polymerization. The chemical composition and microstructural characteristics of the poly(DMAEMA)-grafted EVAL membranes were investigated by attenuated total reflectance Fourier-transform

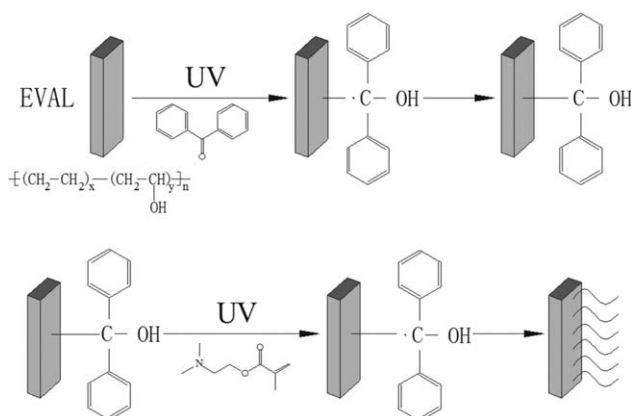


Figure 1. Preparing poly(DMAEMA)-grafted EVAL membrane by UV irradiation graft polymerization.

infrared spectrometer (ATR-FTIR), X-ray photoelectron spectroscopy (XPS), and field-emission scanning electron microscopy (FESEM). The distribution of the grafted chains was investigated by energy-dispersive X-ray spectroscopy (EDX). Atomic force microscopy (AFM) and nitrogen adsorption analysis were used to estimate the surface roughness, surface area, and pore size of the grafted membranes. The surface hydrophilicity, permeability, and selectivity of the membrane were also measured to determine the pH-responsive behavior of membrane under alkaline conditions.

EXPERIMENTAL

Materials

EVAL with an average ethylene content of 38 mol % was purchased from Kuraray (Japan). Dimethylsulfoxide (DMSO), the EVAL solvent, was purchased from Tianyi Chemical Reagents Co. Ltd. (China). DMAEMA (98%) was obtained from J&K Chemicals (Beijing, China) and was purified under depressurized conditions before usage to remove the inhibitor. Benzophenone (BP), which was purchased from Guoyao Chemical Co. Ltd. (Shanghai, China), was used as photoinitiator. The hydrochloric acid (HCl), sodium hydroxide (NaOH), sodium chloride (NaCl), and anhydrous copper sulfate (CuSO_4) were used as analytical reagent grade and obtained from Tianyi Chemical Reagents Co. Ltd. (China).

Preparation of Original EVAL Membrane

The original EVAL membrane was prepared by phase inversion method.²³ EVAL polymer was dissolved in DMSO at 70°C and ultrasonicated for 30 min to eliminate bubbles. Membrane solution was cast on a glass plate and immersed in a water bath at 25°C for membrane formation. The obtained original EVAL membrane was immersed in deionized (DI) water for further modification.

Preparation of Poly(DMAEMA)-Grafted EVAL Membrane

UV irradiation graft polymerization is a useful and versatile technology. It has the following advantages: low operation cost, short reaction time, and feasibility for industrial production.^{24–26} DMAEMA was grafted onto the EVAL membrane using UV irradiation graft polymerization. A UV

illumination system equipped with one high-pressure mercury lamp (400 W with a wavelength range of 232–500 nm) was used. In the first step, EVAL membranes were freeze-dried after removal of impurities by methanol and were subsequently precoated for 2 h in 50 mL acetone solution with a certain amount of BP. In the second step, a certain amount of monomer solution was deposited on the initiator-adsorbed EVAL membranes. The EVAL membranes were placed between two quartz plates and irradiated under UV light for a predetermined time. UV irradiation distance was at 7.5 cm at an intensity of $\sim 7 \text{ mWcm}^{-2}$, as measured by UVA meter from the photoelectric instrument factory of Beijing Normal University. The grafted membranes were subsequently washed with ethanol by Soxhlet extraction for 48 h to remove redundant DMAEMA monomers and poly(DMAEMA) homopolymers.

The grafting degree (*GD*) was calculated according to eq. (1) as follows:

$$GD = \frac{m - m_0}{m_0} \times 100\% \quad (1)$$

Where m_0 and m are the weights of the EVAL membrane and poly(DMAEMA)-grafted EVAL membrane, respectively. Each presented value was the average obtained from three parallel experiments.

Characterization of Membranes

The chemical composition of the original and the poly(DMAEMA)-grafted EVAL membranes was determined using an ATR-FTIR spectrometer (TENSOR37, Bruker AXS) and XPS (K-Aepna, ThermoFisher).

FESEM (S-4800, Hitachi, Japan) and AFM (5500, Agilent) were used to investigate the morphology and surface roughness of the original and the poly(DMAEMA)-grafted EVAL membranes.

EDX analysis was used to examine the distribution of the grafted chains of the membranes. The distribution of the copper element in the membranes was examined by EDX analysis employing the FESEM with a 20 keV energy beam. The membranes were placed in a 40-mL glass bottle and incubated in 10 mL of CuSO_4 solution (2 g/L) for 12 h to reach equilibrium in a shaker bath. Subsequently, the membranes were washed three times with 10 mL of deionized water in a shaker bath. Each washing was performed for 4 h. The membranes were then freeze-dried and fractured in liquid nitrogen for further EDX analysis.

Nitrogen adsorption analysis was used to estimate the surface area and pore size of the membranes. The membranes were characterized by a nitrogen adsorption analyzer (ASAP 2020/Tristar 3000, Micromeritics) at liquid nitrogen temperature. The data were analyzed using the Brunauer–Emmett–Teller (BET) and Barrett–Joyner–Halenda (BJH) models.

Alkali-Responsive Properties

To evaluate the surface hydrophilicity of the poly(DMAEMA)-grafted EVAL membrane surface, a contact angle measurement apparatus (CM3250, KRUSS, Germany) was used to

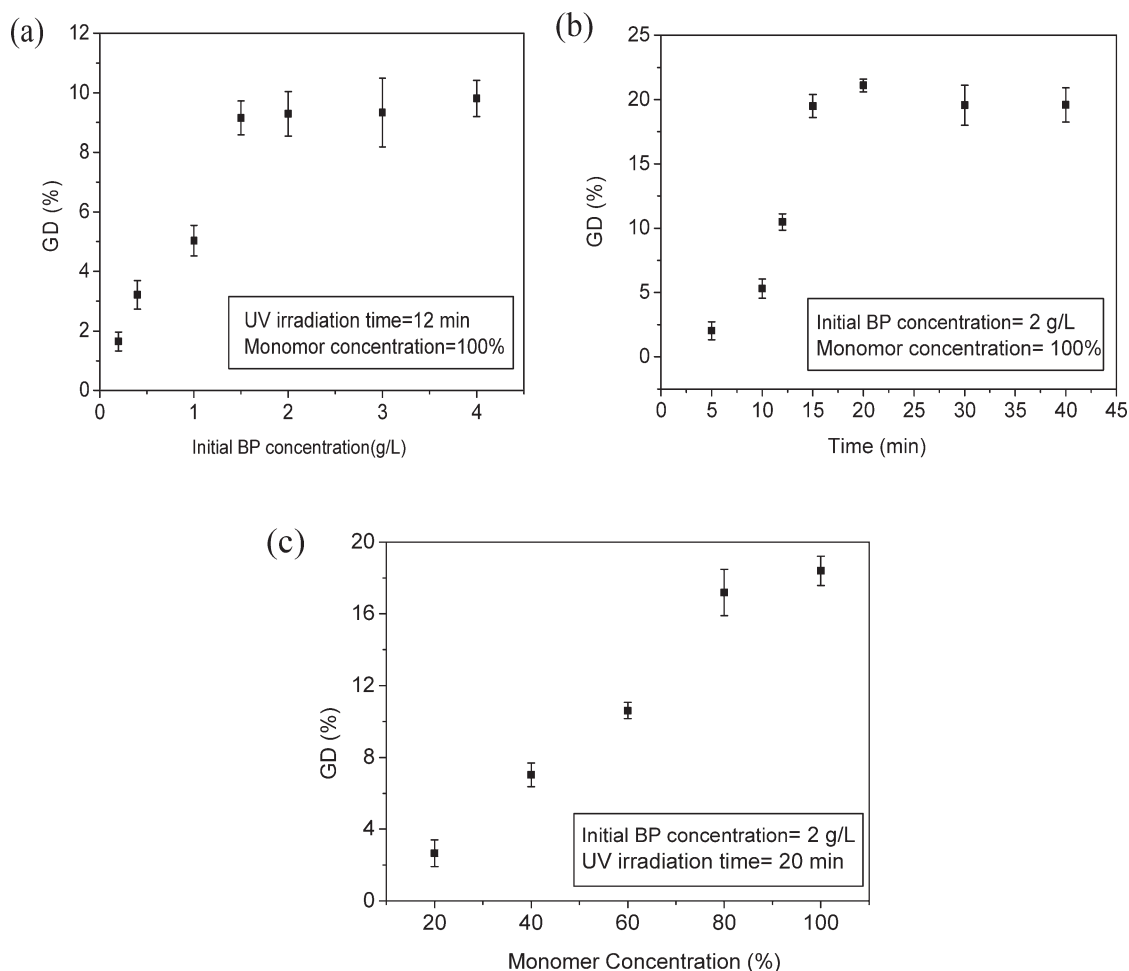


Figure 2. Effect of (a) initial BP concentration, (b) UV irradiation time, and (c) monomer concentration on UV irradiation graft polymerization.

measure the surface contact angles of the original and the poly(DMAEMA)-grafted EVAL membrane.

The permeability of the membrane was determined by measuring the fluxes of the solution through the membrane at different pH values. Permeation experiments on the original and the poly(DMAEMA)-grafted EVAL membranes were conducted using a filtration apparatus with a transmembrane pressure of 0.08 MPa. The pH and salt concentration of the solution were adjusted by adding HCl, NaOH, and NaCl. The pH values of the solution were measured using a pH meter (EL20, Mettler Toledo, Switzerland).

The selectivity was characterized by measuring the rejections of polyethylene glycol10,000 (PEG10,000) and polyethylene glycol20,000 (PEG20,000) at various pH values. The rejections of PEGs were obtained according to eq. (2) as follows:

$$R = \frac{C_1 - C_2}{C_1} \times 100\% \quad (2)$$

Where C_1 and C_2 refer to the PEG concentration of the feed and permeation, respectively. The PEG concentration was determined by the Dragendoff's method²⁷ with a UV-VIS spectrophotometer (UL2100, GE).

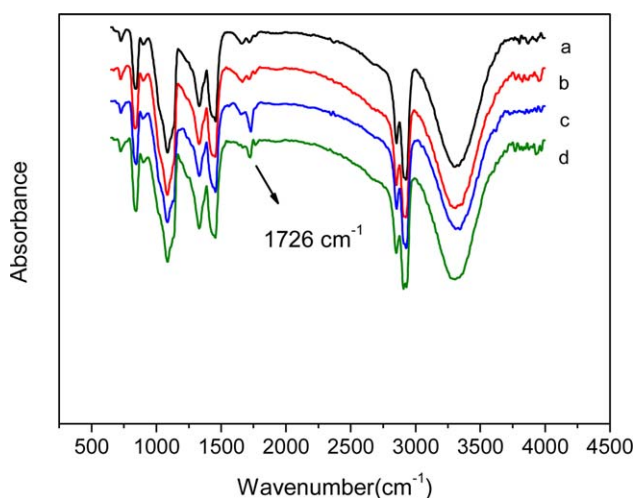


Figure 3. ATR-FTIR spectra of top and back surfaces of the original EVAL membrane (a and b), and top and back surfaces of the poly(DMAEMA)-grafted EVAL membrane with a GD of 19% (c and d). [Color figure can be viewed in the online issue, which is available at wileyonlinelibrary.com.]

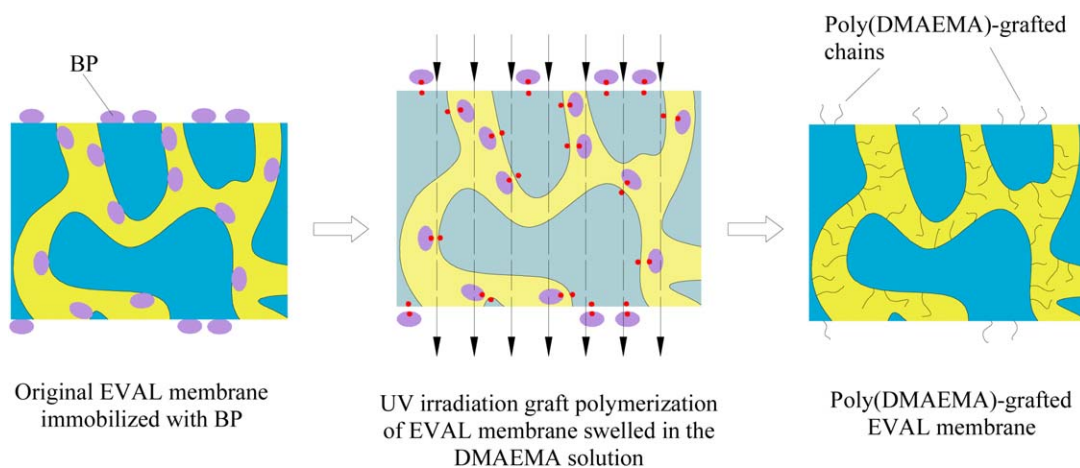


Figure 4. Schematic of UV irradiation graft polymerization for swelled EVAL membrane. [Color figure can be viewed in the online issue, which is available at wileyonlinelibrary.com.]

RESULTS AND DISCUSSION

UV Irradiation Graft Polymerization

Figure 1 shows the general procedure in preparing the poly(DMAEMA)-grafted EVAL membranes. First, photoinitiator BP was adsorbed on the membrane surface and membrane pore walls. Second, UV-initiated “grafting from” of DMAEMA monomers was performed. The BP-adsorbed EVAL membrane was immersed in the DMAEMA solution and irradiated under UV radiation. The UV light cleaved C–C bond of BP and the excited BP abstracted hydrogen from substrates to obtain the radicals used to initiate graft polymerization. The DMAEMA monomers preferentially reacted with the radicals on the membrane surface and membrane pore walls. Meanwhile, homopolymerization in the DMAEMA solution was minimized.

To achieve better control over UV-initiated “grafting from” graft polymerization, we investigated the effects of UV irradiation

conditions, including initial BP concentration, UV irradiation time, and monomer concentration, on the *GD*, and such effects are presented in Figure 2.

At low initial BP concentration (<1.5 g/L), *GD* increased linearly with increasing initial BP concentration (Figure 2a), indicating that the adsorbed density of BP on the membrane surface increased. Such an increase resulted in the generation of initiation sites. However, when the initial BP concentration was more than 1.5 g/L, *GD* changed slowly with the initial BP concentration, showing that the adsorbed density of the BP on the membrane surface was exhibited a tendency to be saturated. Graft density is related to adsorbed density of BP, which indicates that graft density depends on initial BP concentration.

The effect of UV irradiation time on the *GD* of poly(-DMAEMA)-grafted EVAL membrane is shown in Figure 2b. The *GD* increased rapidly with increased UV irradiation time from 5 min to 20 min. The increased production of surface radicals resulted in the accessibility of a large number of DMAEMA monomers to the surface radicals. A growing number of monomers were grafted from the EVAL membrane surface with increasing length of UV irradiation time. However, at a UV irradiation time of longer than 20 min, *GD* increased slowly, which may be due to depletion of the initiator in the reaction system or the material degradation caused by exposure to high-intensity UV irradiation for a long time.

The effect of monomer concentration on the *GD* is illustrated in Figure 2c. The *GD* increased with increased monomer

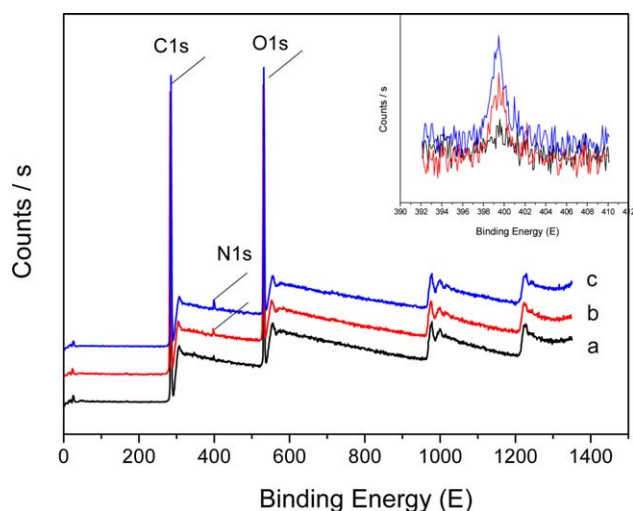


Figure 5. XPS spectra of (a) the original EVAL membrane, (b) the poly(-DMAEMA)-grafted EVAL membrane with a *GD* of 3%, and (c) the poly(-DMAEMA)-grafted EVAL membrane with a *GD* of 19%. [Color figure can be viewed in the online issue, which is available at wileyonlinelibrary.com.]

Table I. Elemental Compositions Obtained from XPS Analysis

Sample	C/(%)	O/(%)	N/(%)
Original EVAL membrane	74.15	24.71	1.14
Poly(DMAEMA)-grafted EVAL membrane with a <i>GD</i> of 3%	73.82	22.03	2.41
Poly(DMAEMA)-grafted EVAL membrane with a <i>GD</i> of 19%	75.13	18.61	4.02

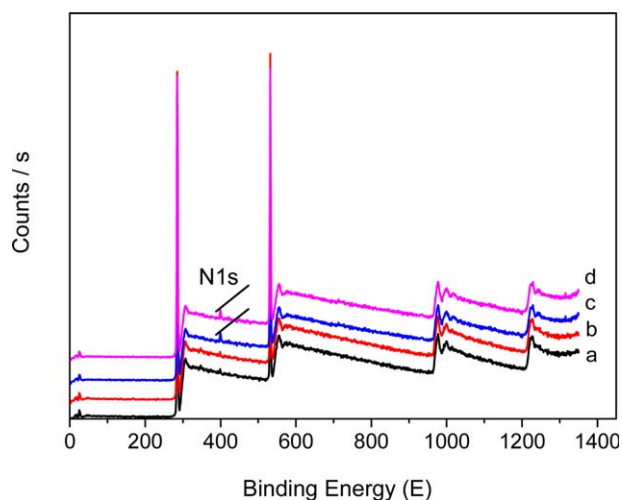


Figure 6. XPS spectra of top and back surfaces of the original EVAL membrane (a and b), and top and back surfaces of the poly(DMAEMA)-grafted EVAL membrane with a *GD* of 19% (c and d). [Color figure can be viewed in the online issue, which is available at wileyonlinelibrary.com.]

concentration. The *GD* was tuned by adjusting the UV-irradiation time and monomer concentration, and such adjustments can potentially benefit the controllable preparation of poly(DMAEMA)-grafted EVAL membranes.

Surface Composition of Membranes

ATR-FTIR. Typical ATR-FTIR spectra are shown in Figure 3. Compared with the ATR-FTIR spectrum of the original EVAL membrane, the poly(DMAEMA)-grafted EVAL membrane had an absorption band centered at 1726 cm^{-1} . Such band corresponded to the carbonyl stretching ($\text{C}=\text{O}$) of poly(DMAEMA) and confirmed the success of the UV irradiation graft polymerization. The poly(DMAEMA)-grafted chains were observed on both top and back surfaces, but the absorption peak intensity on the back was lower than that on the top surface.

This result is distinctly different from those reported in the literature.^{28,29} Yang *et al.*²⁹ developed temperature-responsive membranes by photografting poly(*N*-isopropylacrylamide) (PNIPAAm) on polyester track membranes. PNIPAAm brushes were observed only on membrane surfaces and not inside the pores. Wu *et al.*²⁸ prepared a thermo-sensitive nylon filter membrane. The grafted polymer was observed on the top surface and in the pores rather than on the back probably because the EVAL membrane was slightly swelled in the DMAEMA solution and was in a subtranslucent state, which allowed UV light to pass through all the membrane pores. Thus, graft polymerization in the pores and on the back was induced (Figure 4). The intensity of UV light that can pass through the membranes was 2.2 mWcm^{-2} . Moreover, the absorption peak intensity on the back was lower than that on the top surface because the UV irradiation intensity on the back was significantly lower.

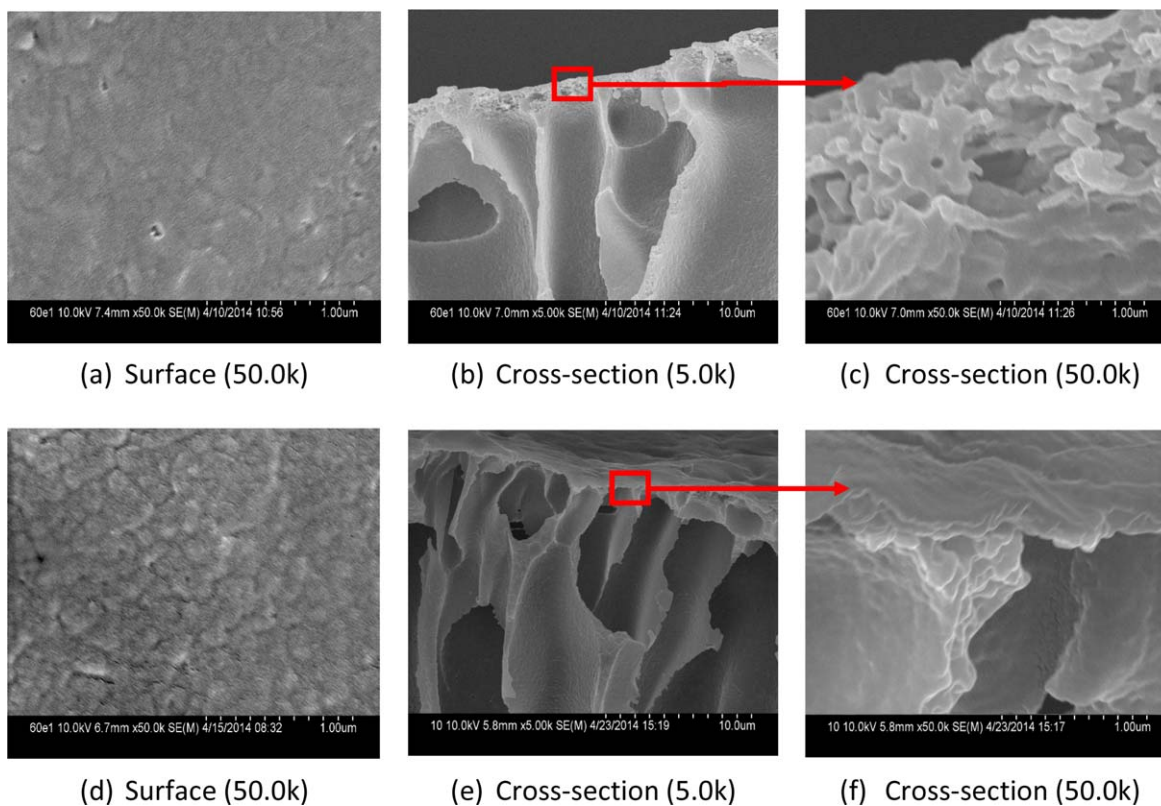


Figure 7. FESEM images of the original EVAL membrane (a–c) and the poly(DMAEMA)-grafted EVAL membrane with a *GD* of 19% (d–f). [Color figure can be viewed in the online issue, which is available at wileyonlinelibrary.com.]

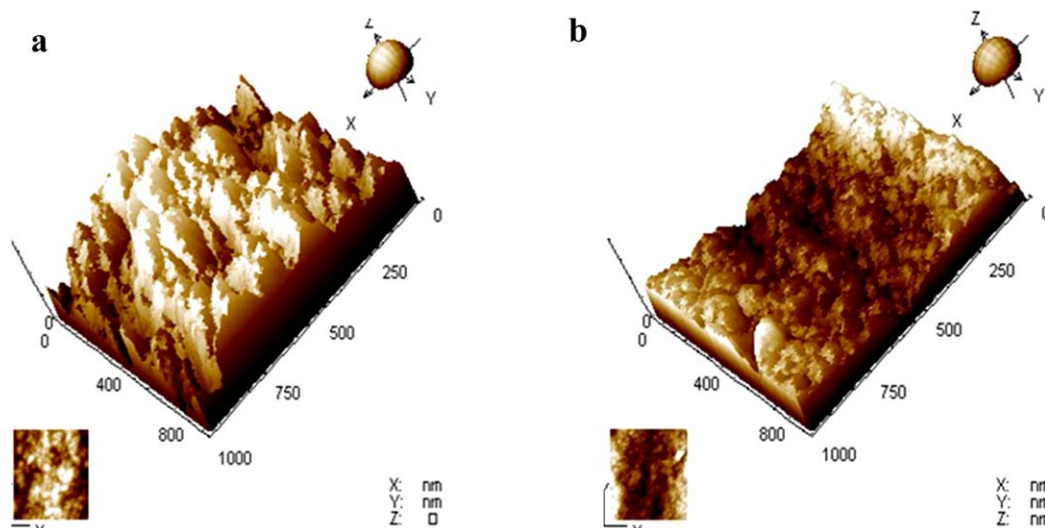


Figure 8. AFM micrographs of (a) the original EVAL membrane and (b) the poly(DMAEMA)-grafted EVAL membrane with a *GD* of 19%. [Color figure can be viewed in the online issue, which is available at wileyonlinelibrary.com.]

XPS. The XPS spectra are depicted in Figure 5, and the elemental compositions obtained from XPS analysis are shown in Table I. A low concentration of nitrogen (N) peak (N 1s) (1.14%) was detected in the original EVAL membrane. N might have originated from the absorbed N from the air. As shown in the inset of Figure 5, the concentration of the N peak (N 1s) in the spectrum of poly(DMAEMA)-grafted EVAL membrane increased with increasing *GD*. According to the data in Table I, the N/C ratio of the original EVAL membrane was 0.015, whereas the nitrogen/carbon (N/C) ratio increased from 0.033 to 0.054 with increasing *GD* from 3% to 19%, indicating that a large number of poly(DMAEMA) chains were grafted onto the membrane.

The XPS spectra of the top and back surfaces of the original EVAL membrane and poly(DMAEMA)-grafted EVAL membrane are depicted in Figure 6. The poly(DMAEMA)-grafted chains were also observed on the back. Graft polymerization occurred on the back, which was consistent with the results obtained by ATR-FTIR.

Morphology of Membranes

FESEM. FESEM was used to observe the morphological changes in the original and the poly(DMAEMA)-grafted EVAL mem-

Table II. EDX Analysis of (a) the Original and (b) the Poly(DMAEMA)-grafted EVAL Membrane

	Sample	Element content (wt %)			
		C	N	O	Cu
Surface	a	78.05	3.16	15.54	3.25
	b	66.70	6.04	17.09	12.15
Cross section	a	64.75	4.12	23.21	7.92
	b	55.31	3.65	18.67	22.37
Back	a	77.69	3.65	14.33	4.33
	b	69.77	4.20	15.33	10.71

brane, as shown in Figure 7. The membrane surface became densely covered with grafted chains after grafting was performed (Figure 7d). As shown by the cross-sectional FESEM images in Figures 7c and 7f, the pore walls of the poly(DMAEMA)-grafted EVAL membrane appeared smoother than the original EVAL membrane. Pore narrowing was observed. The poly(DMAEMA)-grafted chains were grafted inside the membrane pores.

AFM. The surface topography and roughness values of the original and the poly(DMAEMA)-grafted EVAL membrane surfaces were examined by AFM. Figure 8 presents the significant difference in the topography of the original and the poly(DMAEMA)-grafted EVAL membrane with a *GD* of 19%. The surface of the original EVAL membrane was rough, and large-sized peaks and valleys were observed, while the surface

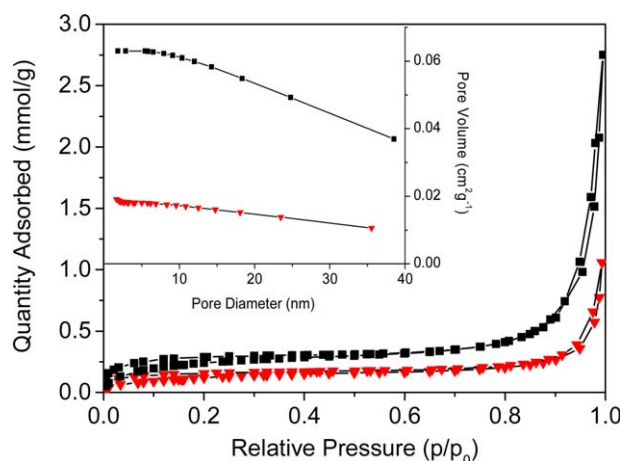


Figure 9. Nitrogen adsorption-desorption isotherm and pore size distributions for (■) the original EVAL membrane and (▼) the poly(DMAEMA)-grafted EVAL membrane with a *GD* of 19%. [Color figure can be viewed in the online issue, which is available at wileyonlinelibrary.com.]

Table III. BET-Specific Surface Area, Pore Volume, and Pore Size of the Membranes

Sample	BET surface area (m^2g^{-1})	BJH desorption cumulative pore volume (cm^3g^{-1})	BJH desorption average pore diameter (nm)
Original EVAL membrane	20.68	0.063	30.52
Poly(DMAEMA)-grafted EVAL membrane with a GD of 19%	10.71	0.019	15.86

of the poly(DMAEMA)-grafted EVAL membrane was smoother and more uniform. The root-mean-square (RMS) was used to evaluate the surface roughness of the membranes. The values of the RMS are decreased from 112.9 nm to 72.86 nm after UV-induced graft polymerization. This finding was attributed to the collapse of the grafted chains in air, which spread uniformly over the surface of the membrane. Consequently, the surface of the original EVAL membrane smoothed, which was similar to the findings of other research groups.³⁰

EDX Analysis

EDX was used to examine the distribution of the grafted chains on the membrane surface and the membrane pore walls. Cu^{2+} ion was adsorbed on the poly(DMAEMA)-grafted chains by complexation action to achieve higher sensitivity.³¹ The N atom of the tertiary amine groups on the poly(DMAEMA)-grafted chains contained a lone pair electron. This N atom possessed the coordination ability with a Cu^{2+} ion. Table II shows the Cu contents on the surface, cross section and back of the membranes before and after UV grafting polymerization. The EDX results indicate that the Cu contents were higher on the surface, cross section, and back of the poly(DMAEMA)-grafted membranes than on the original EVAL membranes. These results provide indirect evidence of the presence of poly(DMAEMA)-grafted chains on the mem-

brane surface and membrane pores. The Cu contents of the original EVAL membrane were possibly due to the nonspecific adsorption of the EVAL materials. In addition, the Cu content on the cross section of the membranes was higher than those on the surface and back of membranes. It may be because the surface area to volume in the membrane pores is higher than on the surface; thus, the Cu^{2+} ion easily accessed the adsorption sites.

BET Analysis

The porous structural parameters of the original and the poly(DMAEMA)-grafted EVAL membranes were measured and shown in Figure 9 and Table III. The BET surface area of the poly(DMAEMA)-grafted EVAL membranes decreased by nearly 50% compared with that of the original EVAL membranes. The grafted polymer chains were also observed within the pores. The collapsed grafted polymer chains spread over the membrane pore walls and decreased the surface area of the grafted membranes.

As shown in Table III, the poly(DMAEMA)-grafted EVAL membranes exhibited lower pore volume and pore size than the original EVAL membranes because of the narrowing of pores.

Alkali-Responsive Properties

Surface Hydrophilicity. The contact angles of the original and the poly(DMAEMA)-grafted EVAL membrane (Figure 10) were used to evaluate the hydrophilicity of the membrane surface.

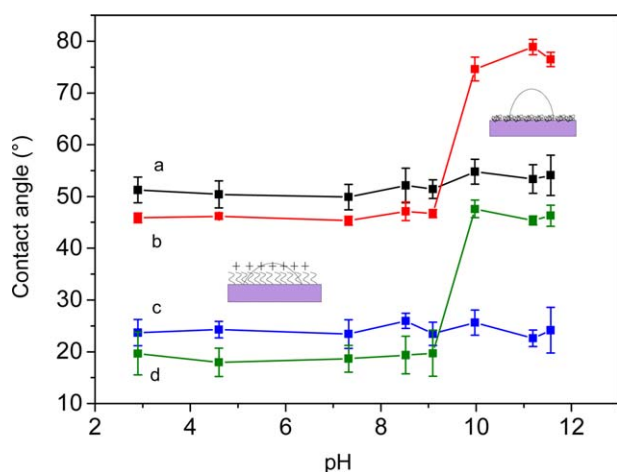


Figure 10. Effect of pH on surface hydrophilicity of top and back surfaces of the original EVAL membrane (a and c), and top and back surfaces of the poly(DMAEMA)-grafted EVAL membrane with a GD of 19% (b and d). [Color figure can be viewed in the online issue, which is available at wileyonlinelibrary.com.]

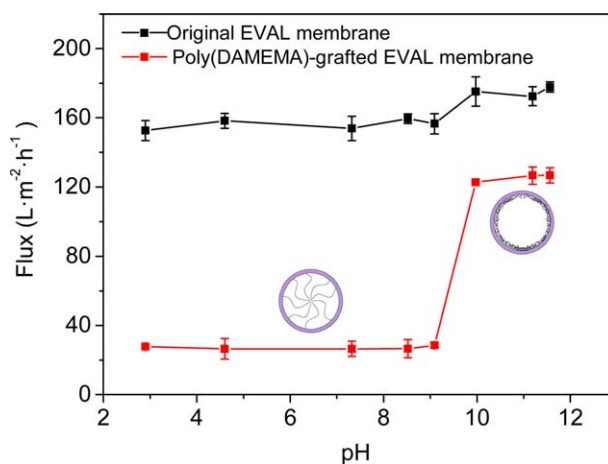


Figure 11. Effect of pH on permeability of the original and the poly(DMAEMA)-grafted EVAL membrane with a GD of 19%. [Color figure can be viewed in the online issue, which is available at wileyonlinelibrary.com.]

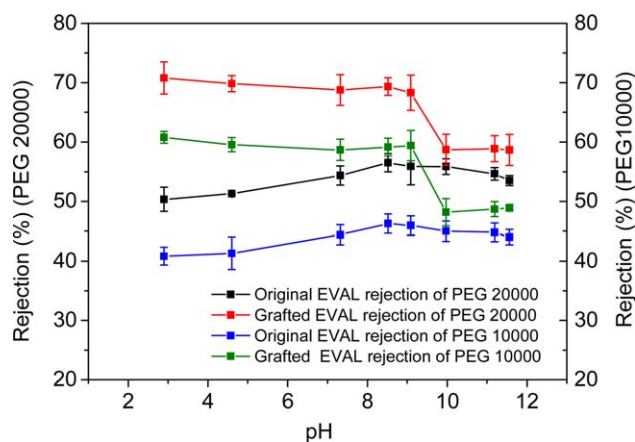


Figure 12. Effect of pH on selectivity of the original and the poly(DMAEMA)-grafted EVAL membrane with a GD of 19%. [Color figure can be viewed in the online issue, which is available at wileyonlinelibrary.com.]

Compared with the original EVAL membrane, the contact angles of the poly(DMAEMA)-grafted EVAL membrane significantly varied according to the environmental pH. A sharp transition of the contact angles occurred with increasing pH from 9 to 10, which corresponded to the pK_a value (approximately 9.2–10) for the tertiary amine group of the DMAEMA³⁰. The amine pendant groups of poly(DMAEMA)-grafted chains on the membrane surface were partially protonated at low pH, resulting in the improvement of hydrophilicity compared with that of the original EVAL membrane. By contrast, poly(DMAEMA)-grafted chains were deprotonated and became more hydrophobic at pH values higher than 10.

As shown in Figure 10, similar pH-dependent results were also obtained at the back of the poly(DMAEMA)-grafted EVAL membrane, and the sharp transition of the contact angles was observed with increasing pH values from 9 to 10.

Permeability. The variation of permeation fluxes was determined to evaluate the permeability of the poly(DMAEMA)-

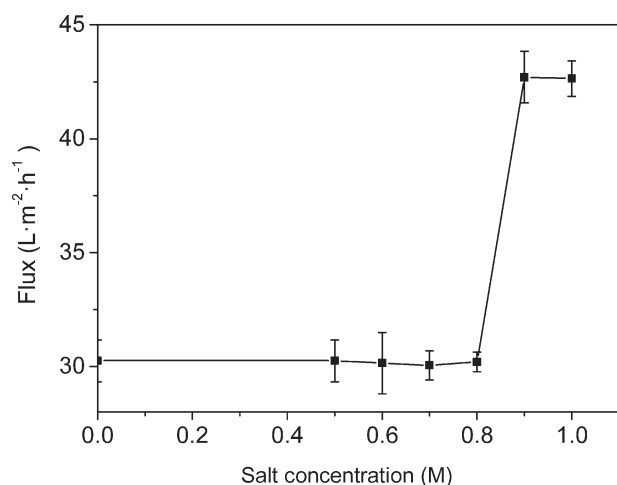


Figure 13. Effect of salt concentration on permeability of the poly(DMAEMA)-grafted EVAL membrane with a GD of 19%.

grafted EVAL membrane, as shown in Figure 11. A dramatic increase in permeation flux was observed at pH values between 9 and 10 because of the variation of the effective membrane pore sizes for transmembrane permeation based on pH change. The poly(DMAEMA)-grafted chains were protonated and hydrophilic below the pK_a . The chains swelled, thereby decreasing the effective pore size of the poly(DMAEMA)-grafted EVAL membrane. By contrast, the poly(DMAEMA)-grafted chains were deprotonated and hydrophobic, and the chains showed deswelling conformation, which increased the effective pore size of the poly(DMAEMA)-grafted EVAL membrane. The on/off switching properties could be used to tune the permeability of the poly(DMAEMA)-grafted EVAL membrane because of conformational changes of the chains at different pH values in the feed solutions. In addition, the permeation fluxes of the poly(DMAEMA)-grafted EVAL membrane were consistently lower than those of the original EVAL membrane even at high pH. It can be explained that the poly(DMAEMA)-grafted chains showed deswelling conformation at high pH but still decreased the pore sizes of the membrane.

The dramatic increase in permeation flux was concentrated in the pH range of 9–10 (Figure 11), indicating that the poly(DMAEMA)-grafted EVAL membrane exhibited a faster pH responsivity than the stimuli-responsive membrane prepared by blending method.^{32,33} The poly(DMAEMA)-grafted chains, which were anchored on the membrane surface and inner pores of the surface, directly participated in pH-responsive activities, thereby improving the speed of pH responsivity.

Selectivity. The rejections of PEG10,000 and PEG20,000 were used to characterize the selectivity of poly(DMAEMA)-grafted EVAL membrane by changing the external pH (Figure 12). The rejection of PEG10,000 of poly(DMAEMA)-grafted EVAL membrane decreased from 60.9% to 48.6% in the pH range of 9–10, suggesting that selectivity could be tuned by changing the external pH. Similar to the results obtained with PEG10,000, the PEG20,000 rejection decreased from 70.9% to 58.8%. However, the decrease in PEG permeation as the pH increased was modest. It can be explained by the following two reasons: (1) although the grafted polymer chains existed within the pores, a low amount of the grafted polymer chains was present within the pores of the separation layer; (2) The membrane pore size distribution was broad. The grafted polymer chains in the membranes were also unevenly distributed. These factors caused inefficient utilization of the on/off switching properties because of the “short circuit” effect. The different pore sizes exhibited different solute residence capacities, and the PEG molecules preferably passed through the less resistant pores instead of passing through “off-state” pores.

Effect of Salt Concentration on Permeability. The effects of salt concentration on the permeability of poly(DMAEMA)-grafted EVAL membranes were also investigated. The flux of the poly(DMAEMA)-grafted EVAL membrane increased sharply from 30.2 $\text{L m}^{-2} \text{h}^{-1}$ to 42.8 $\text{L m}^{-2} \text{h}^{-1}$ by increasing salt concentration from 0.8 M to 0.9 M (Figure 13). The conformation of the poly(DMAEMA)-grafted chains in pH-responsive characteristics was significantly dependent on the dissociation degree of amine pendant groups. When the salt concentration in the

solution was increased, the dissociation degree was minimized because of the effect of charge shielding, which caused the conformation of poly(DMAEMA)-grafted chains to shrink. Thus, the poly(DMAEMA)-grafted chains shrunk sharply with increasing salt concentrations at higher than 0.8 M, thereby increasing the effective pore size.

However, previous investigations have reported that the salt concentration can significantly affect the swelling/deswelling behavior of poly(DMAEMA)-grafted hydrogel at low salt concentration (lower than 0.1 M),^{34,35} a finding that is different from the results of this study. The phenomenon can be explained as follows: poly(DMAEMA)-grafted chains with mobile ends of hydrogel can stretch in the solution, but poly(-DMAEMA)-grafted chains grafted onto the membrane pores walls are in a restrictive state. Thus, the salt concentration response occurs at high salt concentration.

CONCLUSIONS

An alkali-responsive membrane was prepared by grafting DMAEMA onto an EVAL membrane using UV irradiation graft polymerization. The *GD* was tuned by adjusting the conditions of UV irradiation graft polymerization. The results of ATR-FTIR, XPS, FESEM, and EDX indicated that the poly(-DMAEMA)-grafted chains were successfully grafted on the EVAL membrane. The grafted chains existed not only on the top surface but also on the back and inside the membrane pores because of the subtranslucent state of the EVAL membrane, which swelled in the DMAEMA solution. The results of AFM and BET confirmed that the grafted chains collapsed in air, and decreased the surface roughness, surface area, and pore size of the grafted membranes. Alkali-responsive properties of the poly(DMAEMA)-grafted EVAL membranes were observed. A sharp transition of the contact angles occurred under alkaline conditions. Similar results were obtained on the top and back surfaces of the poly(DMAEMA)-grafted EVAL membrane. The changes in permeation flux and rejection of PEG were observed at pH values between 9 and 10. The membrane showed alkali-responsive properties of permeability and selectivity because of the swelling/deswelling of the poly(DMAEMA)-grafted chains in the pores. Moreover, the salt concentration significantly affected permeability. A rapid increase in fluxes was evident when salt concentration increased from 0.8 M to 0.9 M.

ACKNOWLEDGMENTS

This research was sponsored by the National Natural Science Foundation of China (Funding No. 51373120, No. 51173132), the Research Fund for the Doctoral Program of Higher Education (Funding No. 20111201110003) the Program for Changjiang Scholars and Innovative Research Team in University (PCSIRT) of Ministry of Education of China (No. IRT13084), Tangshan City science and technology research and development program (131302116a).

REFERENCES

1. Zhao, C.; Nie, S.; Tang, M.; Sun, S. *Prog. Polym. Sci.* **2011**, *36*, 1499.
2. Wandera, D.; Wickramasinghe, S. R.; Husson, S. M. *J. Membr. Sci.* **2010**, *357*, 6.
3. Chen, Y. C.; Xie, R.; Chu, L. Y. *J. Membr. Sci.* **2013**, *442*, 206.
4. Hsu, C. C.; Wu, C. S.; Liu, Y. L. *J. Membr. Sci.* **2014**, *450*, 257.
5. Chu, L. Y.; Li, Y.; Zhu, J. H.; Wang, H. D.; Liang, Y. J. *J. Control. Release.* **2004**, *97*, 43.
6. Mi, P.; Ju, X. J.; Xie, R.; Wu, H. G.; Ma, J.; Chu, L. Y. *Polymer* **2010**, *51*, 1648.
7. Mika, A. M.; Childs, R. E.; Dickson, J. M. *J. Membr. Sci.* **1999**, *153*, 45.
8. Hu, K.; Dickson, J. M. *J. Membr. Sci.* **2007**, *301*, 19.
9. Chen, Y. C.; Xie, R.; Chu, L. Y. *J. Membr. Sci.* **2013**, *442*, 206.
10. Li, L.; Xiang, T.; Su, B.; Li, H.; Qian, B.; Zhao, C. *J. Appl. Polym. Sci.* **2012**, *123*, 2320.
11. Alibhai, Z.; Mondor, M.; Moresoli, C.; Ippersiel, D.; Lamarche, F. *Desalination* **2006**, *191*, 351.
12. Ding, X.; Zhu, F.; Gao, S. *Food Chem.* **2012**, *131*, 677.
13. Qiu, X.; Ren, X.; Hu, S. *Carbohydr. Polym.* **2013**, *92*, 1887.
14. Tomicki, F.; Krix, D.; Nienhaus, H.; Ulbricht, M. *J. Membr. Sci.* **2011**, *377*, 124.
15. Zhao, J.; Song, L.; Shi, Q.; Luan, S.; Yin, J. *ACS Appl. Mater. Interfaces.* **2013**, *5*, 5260.
16. Cai, Y.; Li, J.; Guo, Y.; Cui, Z.; Zhang, Y. *Desalination* **2011**, *283*, 25.
17. Avramescu, M. E.; Sager, W. F. C.; Wessling, M. *J. Membr. Sci.* **2003**, *216*, 177.
18. Tetala, K. K. R.; Skrzypek, K.; Levisson, M.; Stamatialis, D. *F. Sep. Purif. Technol.* **2013**, *115*, 20.
19. Li, Y. C.; Liao, Y. T.; Chang, H. H.; Young, T. H. *Colloids Surf. B.* **2013**, *102*, 53.
20. Young, T. H.; Hu, W. W. *Biomaterials* **2003**, *24*, 1477.
21. Yao, C. H.; Chuang, W. Y.; Chen, Y. S.; Young, T. H. *Mater. Chem. Phys.* **2002**, *73*, 1.
22. Young, T. H.; Chuang, W. Y.; Wei, C. W.; Tang, C. Y. *J. Membr. Sci.* **2001**, *191*, 199.
23. Avramescu, M. E.; Sager, W. F. C.; Mulder, M. H. V.; Wessling, M. *J. Membr. Sci.* **2002**, *210*, 155.
24. Chao Zhou, H. W. Z.; Yan Jiang; Wen-Jun Wang; Qiang Yu. *J. Appl. Polym. Sci.* **2011**, *121*, 1254.
25. Deng, J.; Wang, L.; Liu, L.; Yang, W. *Prog. Polym. Sci.* **2009**, *34*, 156.
26. Yu, H. Y.; Zhou, J.; Gu, J. S.; Yang, S. *J. Membr. Sci.* **2010**, *364*, 203.
27. Han, J.; Yang, D.; Zhang, S.; Jian, X. *J. Membr. Sci.* **2009**, *345*, 257.
28. Wu, G.; Li, Y.; Han, M.; Liu, X. *J. Membr. Sci.* **2006**, *283*, 13.
29. Yang, B.; Yang, W. *J. Membr. Sci.* **2003**, *218*, 247.

30. Bhut, B. V.; Wickramasinghe, S. R.; Husson, S. M. *J. Membr. Sci.* **2008**, *325*, 176.
31. Baojian Gao, Y. C.; Zhenguo Zhang *Appl. Surf. Sci.* **2010**, *257*, 254.
32. Huang, R.; Kostanski, L. K.; Filipe, C. D. M.; Ghosh, R. *J. Membr. Sci.* **2009**, *336*, 42.
33. Xue, J. L. C.; Wang, H. L. *Langmuir* **2008**, *24*, 14151.
34. Deng, L.; Zhai, Y.; Lin, X.; Jin, F.; He, X.; Dong, A. *Eur. Polym. J.* **2008**, *44*, 978.
35. Huang, Y.; Liu, M.; Wang, L.; Gao, C.; Xi, S. *React. Funct. Polym.* **2011**, *71*, 666.